

Molecular Dynamics Study of a New Metastable Allotropic Crystalline Form of Gallium—Supertetrahedral Gallium

Iliya V. Getmanskii ^[a], Vitaliy V. Koval ^[a], Alexander I. Boldyrev ^{*,[a,b]},
Ruslan M. Minyaev ^{*,[a]} and Vladimir I. Minkin ^[a]

A new metastable crystalline form of gallium has been computationally designed using density functional calculations with imposing periodic boundary conditions. The geometric and electronic structures of the predicted new allotrope were calculated on the basis of a diamond lattice in which all carbon atoms are replaced by gallium Ga₄ tetrahedra. This form does not have any imaginary phonons, thus it is a metastable crystalline form of gallium. The new form of gallium is a metal and shows high plasticity and low-melting temperature. Molecular dynamics simulations show that this form of gallium will melt at about 273 K with a sharp increase

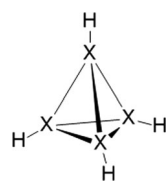
in temperature in the system during the melting process from 273 to 1800 K. This melting process is very different from conventional melting, where temperature stays the same until complete melting. That unusual melting can be explained by the fact that supertetrahedral gallium is a metastable structure that has an excess of strain energy released during melting. If made this new material may find many useful applications as a new low density metal with stored internal energy. © 2019 Wiley Periodicals, Inc.

DOI: 10.1002/jcc.25837

Introduction

The rapid progress of science and technology constantly requires development of new materials with specific properties. In this respect, computational design provides relatively quick and low-cost assessment of the structure and properties of new materials plays an indispensable role.^[1–8] Metastable materials are a new area of research that offers almost an infinite number of new materials with unusual and unexpected properties.^[9–12]

Back in 1985 Burdett and Lee^[13] noted that a carbon atom in the crystal lattice of a diamond can be replaced by a carbon tetrahedron C₄ without loss of symmetry and periodicity of the crystal, and thus proposed a new allotropic form of carbon. Similarly, a new allotropic form of carbon can be obtained by replacing a carbon atom in the diamond lattice by the C₈ cube^[14] and other stable polyhedral structures.^[3] More than a quarter of a century ago, a group of Chinese authors^[15a] published solid-state calculations of the geometric and physical properties of supertetrahedral diamond (T-carbon). T-carbon was experimentally realized in 2017.^[15b] According to quantum chemical calculations, the T_d structure **1** (X = B) B₄H₄ is kinetically stable despite the electron deficit in the system excluding formation of two-center two-electron (2c–2e) bonds between all atoms.^[16,17] Therefore, boron tetrahedron is also could be used as a structural unit for the design of tetrahedral crystalline structures.^[7,8] Both aluminum and gallium tetrahedrons: Al₄H₄ and Ga₄H₄^[16] correspond to a global minimum on the potential energy surface (PES).



1 (X = B, Al, Ga) T_d

Thus, the sufficiently high stability of tetrahedral structures **1** for boron, carbon, aluminum, silicon, and gallium compounds suggests the possibility of the solid-state structures based on these X₄ tetrahedra. Expected sufficient kinetic stability of these metastable solids opens a possibility for new interesting physical properties (hardness, plasticity, electrical conductivity, etc.). Most importantly, new supertetrahedral materials are extremely light and that opens new potential application for these substances. Indeed, calculations of supertetrahedral structures of solid boron and aluminum showed^[7,18] that they possess dynamic stability and have amazingly low density with some of them being below the water density, as well as sufficiently high plasticity and elastic properties.

In this article, the geometric and electronic structure of solids designed on the basis of a diamond lattice in which carbon atoms are replaced by gallium and indium tetrahedron **1** (X = Ga, In) are investigated using quantum chemical calculations with imposing periodic boundary conditions.

Computational Details

We initially performed a machine search for the global minimum structure for the Ga₄H₄ stoichiometry. We used the Coalescence-Kick method^[19] and Gaussian 09 program^[20] for

[a] I. V. Getmanskii, V. V. Koval, A. I. Boldyrev, R. M. Minyaev, V. I. Minkin
Institute of Physical and Organic Chemistry, Southern Federal University,
344090, Rostov-on-Don, Russian Federation
E-mail: a.i.boldyrev@usu.edu or minyaev@ipoc.sfedu.ru

[b] A. I. Boldyrev
Department of Chemistry and Biochemistry, Utah State University, Logan,
Utah
E-mail: a.i.boldyrev@usu.edu

Contract Grant sponsor: National Science Foundation USA; Contract Grant number: CHEM-1664379; Contract Grant sponsor: Russian Government grant by decree N 220 ; Contract Grant number: № 14.Y26.31.0016

© 2019 Wiley Periodicals, Inc.

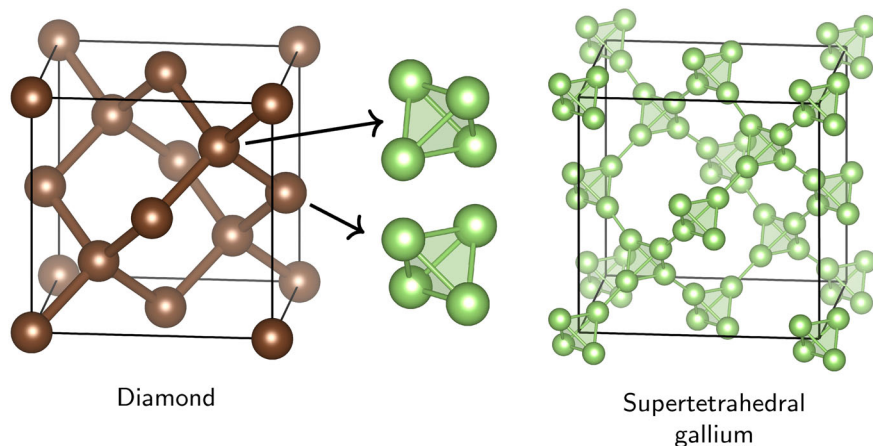


Figure 1. Schematic representation of a cubic unit cell of the crystal structure of supertetrahedral gallium (on the right) and its design from the lattice of diamond by replacing the carbon atoms with gallium tetrahedra (left). [Color figure can be viewed at wileyonlinelibrary.com]

the search. Calculations were performed at the PBE0/LANL2DZ level^[21,22] (12,000 initial structures). After that the lowest structures were reoptimized at the PBE0/aug-cc-pvTZ level of theory and finally single point calculations at the PBE0/aug-cc-pvTZ^[23] geometry were calculated at the CCSD(T)/aug-cc-pvTZ level of theory.^[24] We confirmed that the tetrahedral Ga₄H₄ structure containing the Ga₄ core cluster is indeed the global minimum structure in agreement with the previous results.^[16] However, at our highest level of theory (CCSD(T)/aug-cc-pvTZ), the tetrahedral structure is more stable than the second isomer by 6.5 kcal/mol, which is appreciably higher than in the previous work (0.3 kcal/mol). Thus the preference of the tetrahedral structure over all other structures is now well-established.

Solid-state calculations for supertetrahedral structures of Ga and In were carried out using Vienna Ab initio Simulations Package^[25–28] with projector augmented wave (PAW) pseudopotentials^[29,30] and the PBEsol density functional.^[31] The plane-wave cutoff energy of 340 eV of the associated pseudopotentials was used. The Brillouin zone has been sampled by the Monkhorst-Pack^[32] method with an automatic generated grid of 15 × 15 × 15. The crystal structure was visualized using VESTA software package.^[33]

Molecular dynamics simulation of homogeneous melting of supertetrahedral gallium was performed at constant number of particles, constant volume, and constant total energy (micro-canonical or NVE ensemble). The computational supercell was obtained as 2 × 2 × 2 face-centered cubic primitive cells involving 64 atoms. A time step of 0.4 fs was used for the integration of Newton's equations of motion. The initial positions of the ions correspond to the *cF*-Ga₈ crystal structure. The initial velocities of the ions are set randomly according to a Maxwell-Boltzmann distribution at the initial temperature. Simulations were performed at initial temperatures of 530, 540, and 550 K. Simulations were run for 35 ps.

Results and Discussion

The *cF*-Ga₈ structure has a face-centered cubic lattice (space group *Fd3m*, number 227) with eight gallium atoms per primitive unit cell, which is presented in Figure 1. Cartesian coordinates of translational vectors and coordinates of atoms in the unit cell are given in Supporting Information.

The lattice constant of *cF*-Ga₈ is 12.874 Å. Gallium atoms occupy Wyckoff position 32e, which has coordinates (0.07040, 0.07040, 0.07040). The length of the intertetrahedral covalent Ga–Ga bond is 2.435 Å. This value is smaller than the length of such bond in the tetrahedral gallium dimer (2.512 Å) calculated at the PBE0/6-311+G** level of theory. Such a decrease in the intertetrahedral bond in a solid as compared to an isolated dimer can be explained by packaging effects.

To understand chemical bonding in the supertetrahedral gallium, we run calculations for a model (Ga₄H₃)₂ dimer at the PBE0/6-311+G** level of theory, which contains all important bonding elements. We used the natural bonding orbital (NBO) analysis^[34] for deciphering chemical bonding in this cluster. We found that four gallium atoms in the same tetrahedron are bound together by four three-center two-electron (3c–2e) bonds. The distance between two Ga atoms in the same tetrahedron is

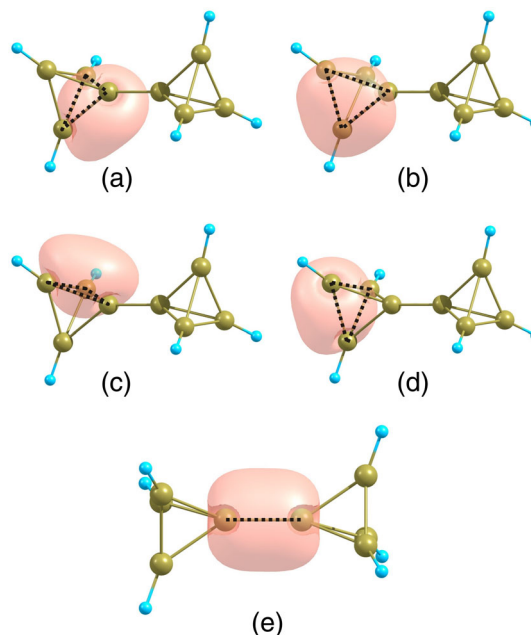


Figure 2. a–d) NBO orbitals corresponding to 3c–2e bonds in one tetrahedron of the (Ga₄H₃)₂ dimer. Dashed lines show the face to which belong gallium atoms connected by three-center two-electron bonds; e) NBO orbital corresponding to 2c–2e intertetrahedral bond in (Ga₄H₃)₂ dimer. [Color figure can be viewed at wileyonlinelibrary.com]

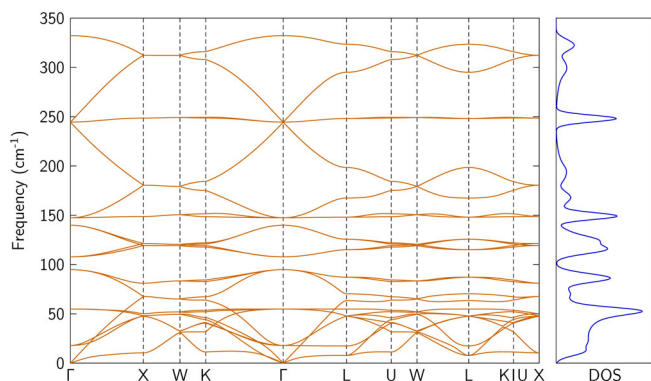


Figure 3. Calculated phonon dispersion curves along high-symmetry lines in the first Brillouin zone (left panel) and phonon density of states (right panel) for *cF*-Ga₈. [Color figure can be viewed at [wileyonlinelibrary.com](#)]

2.565 Å, which is larger than the Ga–Ga intertetrahedral distance. This could be explained by the fact that the intertetrahedral bond is as a classical two-center two-electron (2c–2e) covalent bond, while an intratetrahedral Ga–Ga bond is the 3c–2e bond (see Fig. 2 below NBO in model (Ga₄H₃)₂ molecule).

The calculated density of the supertetrahedral gallium is equal to 1.74 g/cm³, which is considerably lower than that of the usual structure of gallium 5.9 g/cm³, but it is higher the density of supertetrahedral aluminum (0.61 g/cm⁻³),^[18] supertetrahedral boron (0.92 g/cm⁻³),^[7] and T carbon (1.50 g/cm⁻¹).^[15] The calculated phonon spectrum is shown in Figure 3.

There are no low-frequency branches entering into the imaginary region. This finding indicates that the crystal structure is dynamically stable. The bulk, shear, and Young's modules of polycrystalline *cF*-Ga₈ are 11.05, 2.95, and 8.12 GPa, respectively, and its Poisson's ratio is 0.3776. The elastic properties of supertetrahedral gallium are similar to those of supertetrahedral aluminum.^[18]

The calculated electronic band structure is shown in Figure 4. The band gap is absent, that is, *cF*-Ga₈ as the supertetrahedral aluminum, is a good electric conductor. (However, it is worth noting that density functional theory (DFT) methods may underestimate the band gap^[35b] by 3–50%). The calculated plots of the real and imaginary parts of the complex dielectric constant versus the photon energy are shown in Figure 5. The

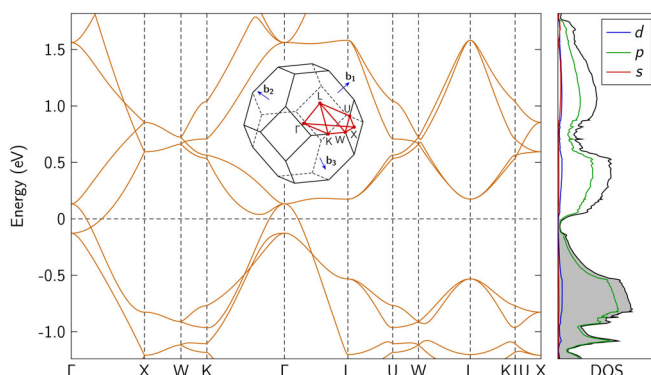


Figure 4. Calculated electronic band structure along high-symmetry lines in the first Brillouin zone (left panel) and electronic full (black line) and partials (color lines) densities of states (right panel) for *cF*-Ga₈. [Color figure can be viewed at [wileyonlinelibrary.com](#)]

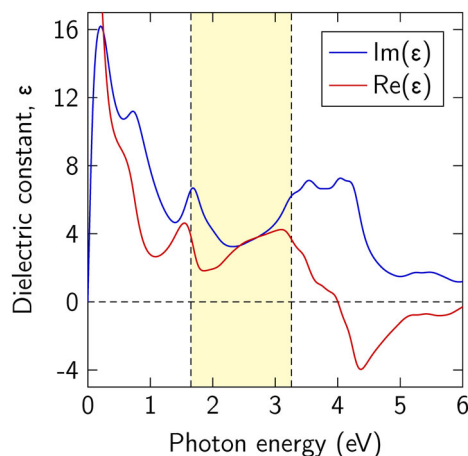


Figure 5. Frequency dependence of the real (red curve) and imaginary (blue curve) parts of complex dielectric permittivity for *cF*-Ga₈. [Color figure can be viewed at [wileyonlinelibrary.com](#)]

minimum absorption is observed at 535 nm (2.32 eV) in the green region of the spectrum.

Similar solid-state calculations for the supertetrahedral indium crystal reveal that this solid is not kinetically stable, because it has imaginary phonons for the optimal structure. Therefore, we will not discuss this substance any further. Instability of the supertetrahedral indium could be due to the fact, that unlike Al₄H₄ and Ga₄H₄, In₄H₄ is not a global minimum on the PES.^[16] The global minimum structure for In₄H₄ is the tetrahedral structure with H atoms located over the center of the four faces. Also, In₄H₄ structures with broken tetrahedra are more stable.

To evaluate the thermodynamic stability of the supertetrahedral gallium, we performed molecular dynamics simulation of it. Figure 6 shows the obtained curves of the change in the instantaneous temperature in the system with time for two values of the initial temperature. At the initial temperature of 540 K, the instantaneous temperature in the system fluctuates around an average value of 270 K and during this time no melting occurs. The behavior of the system was analyzed for 35 ps. At the initial temperature of 550 K, the instantaneous temperature in the system during the first 16 ps fluctuates around the mean value of 273 K. After that the melting process occurs during 4 ps, in which the temperature in the system increases sharply to 1800 K and then oscillates near this mean value. This

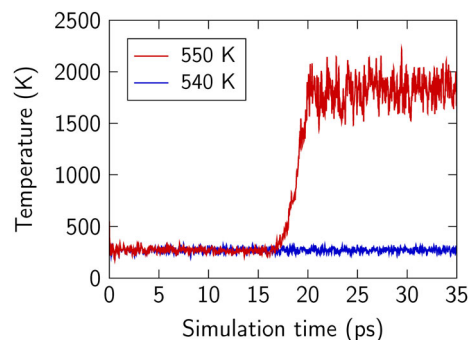


Figure 6. Time evolution of the instantaneous temperature for the system at initial temperatures of 540 K (blue curve) and 550 K (red curve). [Color figure can be viewed at [wileyonlinelibrary.com](#)]

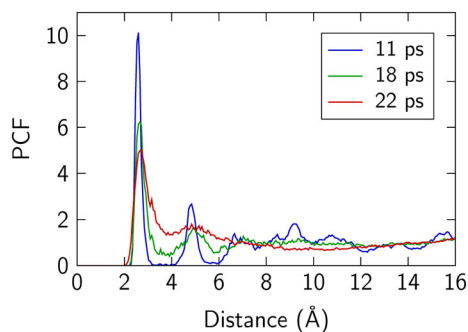


Figure 7. Evolution with time of the pair-correlation function from molecular dynamics simulation at initial temperature of 550 K. [Color figure can be viewed at wileyonlinelibrary.com]

melting process is very different from conventional melting, where temperature stays the same until complete melting. Such a sharp increase in temperature in the system during the melting process can be explained by the fact that supertetrahedral gallium is a metastable structure that has an excess of strain energy released during melting (the cohesive energy per atom of supertetrahedral gallium, 2.33 eV, is about 0.5 eV less than the cohesive energy of α -gallium^[35a]).

Figure 7 shows the graphs of the pair correlation function (PCF) calculated for three instants of time. The graph corresponding to a time point of 11 ps from the start of the simulation is a typical PCF for the crystal. A graph corresponding to a time point of 22 ps has the form of a PCF characteristic of a liquid. The graph corresponding to a time of 18 ps has the appearance intermediate between the PCF of the crystal and the liquid.

Figure 8 shows the time evolution of the root-mean-square deviation of atoms from their equilibrium positions. It can be seen that during the first 16 ps the RMSD function oscillates near zero, which is typical for a crystal, and then the values of this function begin to increase sharply, which corresponds to beginning of the melting process. In general, we can conclude that the melting temperature of supertetrahedral gallium according to our calculations is about 273 K that is considerably lower than that usual melting temperature of gallium 302.93 K.^[36]

To compare the melting processes of supertetrahedral gallium and ordinary gallium, calculations of molecular dynamics simulation of α -gallium were carried out. The melting process of α -gallium is similar to the melting of ordinary substances. For

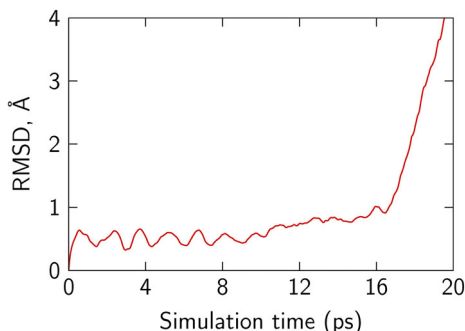


Figure 8. Time dependence of the root-mean-square deviation of the atoms relative to their equilibrium positions in the crystal lattice of supertetrahedral gallium. [Color figure can be viewed at wileyonlinelibrary.com]

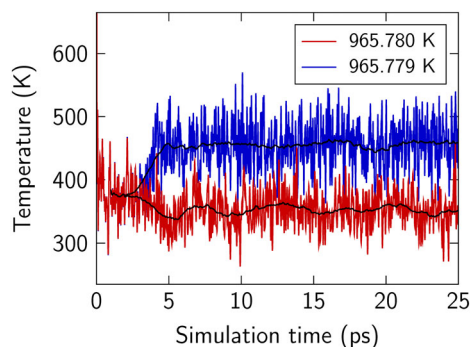


Figure 9. Time evolution of the instantaneous and time-averaged temperature for the α -gallium at initial temperatures of 965.779 K (blue curve) and 965.780 K (red curve). [Color figure can be viewed at wileyonlinelibrary.com]

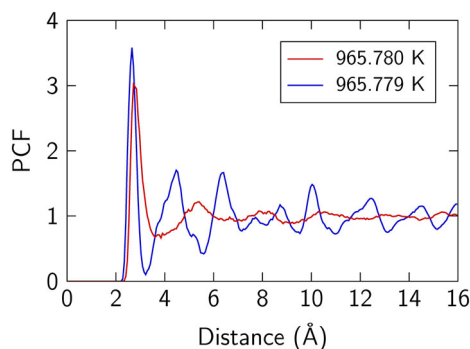


Figure 10. The pair-correlation function for the α -gallium from molecular dynamics simulations at initial temperatures of 965.779 K (blue curve) and 965.780 K (red curve). The graphs correspond to a time point of 24 ps from the start of the simulation. [Color figure can be viewed at wileyonlinelibrary.com]

comparison in Figures 9 and 10 show the results of molecular dynamics simulations of a homogeneous melting of an α -gallium sample, performed at constant number of particles (64 atoms), constant volume, and constant total energy.

At an initial temperature of 965.779 K, melting does not occur, the sample remains in the superheated solid state at an average temperature of about 460 K (Fig. 9). The graph of the pair-correlation function (Fig. 10) confirms that the sample remains in a solid state. At a slightly higher initial temperature, 965.780 K, already after 2 ps from the beginning of the simulation, homogeneous melting of the sample begins, accompanied by a drop in its average temperature to 350 K as the latent heat is removed from the kinetic energy (Fig. 9). The graph of the pair-correlation function (Fig. 10) confirms that the sample becomes liquid. Note that, according to the Z-method,^[37] this temperature (350 K) should be considered the melting point of α -gallium.

Conclusions

In summary, we designed a new form of gallium allotrope constructed on the basis of a diamond lattice in which carbon atoms are replaced by gallium Ga_4 tetrahedra. Follow-up quantum chemical calculations confirmed that the three-dimensional supertetrahedral gallium crystal structure represents a metastable low-density (1.74 g/cm^3) phase of gallium. The new material is an electric conductor with high plasticity. Molecular dynamics calculations show that this metastable material is stable as a


crystal up to 273 K. At this temperature, it melts with sharp increase of temperature from 273 to 1800 K, which is not observable in conventional melting, where temperature stays the same until complete melting. This unusual behavior can be understood on basis of the metastable nature of the super-tetrahedral gallium. If made this new material may find many useful applications as a new low density metal with stored internal energy. Our calculations show that the supertetrahedral indium is not kinetically stable.

Acknowledgment

The work was supported by the Russian Government grant by decree N 220 (agreement № 14.Y26.31.0016) and by the USA National Science Foundation (grant CHEM-1664379) to AIB. The authors greatly appreciate help from Natalia M. Boldyreva and Nikita Fedik with the global minimum search calculations of the Ga_4H_4 cluster and follow up high level of theory calculations.

Keywords: molecular dynamics · gallium melting · gallium · supertetrahedral gallium

How to cite this article: I. V. Getmanskii, V. V. Koval, A. I. Boldyrev, R. M. Minyaev, V. I. Minkin. *J. Comput. Chem.* **2019**, *40*, 1861–1865. DOI: 10.1002/jcc.25837

 Additional Supporting Information may be found in the online version of this article.

- [1] J. Neugebauer, T. Hickel, *WIREs Comput. Mol. Sci.* **2013**, *3*, 301.
- [2] C. Draxl, D. Nabok, K. Hannewald, *Acc. Chem. Res.* **2014**, *47*, 3225.
- [3] V. Georgakilas, J. A. Perman, J. Tucek, R. Zboril, *Chem. Rev.* **2015**, *115*, 4744.
- [4] L. Colombo, A. Fasolino, Eds., *Computer-Based Modeling of Novel Carbon Systems and Their Properties: Beyond Nanotubes*, Springer, Heidelberg, **2010**, p. 258.
- [5] F. Diederich, Y. Rubin, *Angew. Chem. Int. Ed. Engl.* **1992**, *31*, 1101.
- [6] F. Diederich, M. Kivala, *Adv. Mater.* **2010**, *22*, 803.
- [7] I. V. Getmanskii, R. M. Minyaev, D. V. Steglenko, V. V. Koval, S. A. Zaitsev, V. I. Minkin, *Angew. Chem. Int. Ed.* **2017**, *56*, 10118.
- [8] R. M. Minyaev, I. V. Getmanskii, V. I. Minkin, *Russ. J. Inorg. Chem.* **2014**, *59*, 332 Zh. Neorg. Khim. 2014, *59*, 487.
- [9] W. Sun, S. T. Dacek, S. P. Ong, G. Hautier, A. Jain, W. D. Richards, A. C. Gamst, K. A. Persson, G. Ceder, *Sci. Adv.* **2016**, *2*, e1600225.
- [10] R. Quesada Cabrera, A. Sella, E. Bailey, O. Leynaud, P. F. McMillan, *J. Solid State Chem.* **2011**, *184*, 915.
- [11] W. Zhang, A. R. Oganov, A. F. Goncharov, Q. Zhu, S. E. Boulfelfel, A. O. Lyakhov, E. Stavrou, M. Somayazulu, V. B. Prakapenka, Z. Konôpková, *Science* **2013**, *342*, 1505.
- [12] X. Dong, A. R. Oganov, A. F. Goncharov, E. Stavrou, S. Lobanov, G. Saleh, G.-R. Qian, Q. Zhu, C. Gatti, V. L. Deringer, R. Dronskowski, X.-F. Zhou, V. B. Prakapenka, Z. Konôpková, I. A. Popov, A. I. Boldyrev, H.-T. Wang, *Nature Chem.* **2017**, *9*, 440.
- [13] J. K. Burdett, S. Lee, *J. Am. Chem. Soc.* **1985**, *107*, 3063.
- [14] R. L. Johnston, R. Hoffmann, *J. Am. Chem. Soc.* **1989**, *111*, 810.
- [15] (a) X. L. Sheng, Q. B. Yan, F. Ye, Q. R. Zheng, G. Su, *Phys. Rev. Lett.* **2011**, *106*, 155703. (b) J. Zhang, R. Wang, X. Zhu, A. Pan, C. Han, X. Li, D. Zhao, C. Ma, W. Su, C. C. Niu, *Nat. Commun.* **2017**, *8*, 683.
- [16] R. Haunschild, G. Frenking, *Mol. Phys.* **2009**, *107*, 911.
- [17] J. K. Olson, A. I. Boldyrev, *Chem. Phys.* **2011**, *379*, 1.
- [18] I. V. Getmanskii, V. V. Koval, R. M. Minyaev, A. I. Boldyrev, V. I. Minkin, *J. Phys. Chem. C* **2017**, *121*, 22187.
- [19] A. P. Sergeeva, B. B. Averkiev, H. J. Zhai, A. I. Boldyrev, L. S. Wang, *J. Chem. Phys.* **2011**, *134*, 224304.
- [20] M. J. Frisch, et al., Gaussian09 (Revision B.0.1), Gaussian, Wallingford, CT, **2009**.
- [21] C. Adamo, V. Barone, *J. Chem. Phys.* **1999**, *110*, 6158.
- [22] J. Hay, W. R. Wadt, *J. Chem. Phys.* **1985**, *82*, 270.
- [23] R. A. Kendall, T. H. Dunning, Jr., R. J. Harrison, *J. Chem. Phys.* **1992**, *96*, 6796.
- [24] (a) G. D. Purvis, R. J. Bartlett, *J. Chem. Phys.* **1982**, *76*, 1910. (b) K. Raghavachari, G. W. Trucks, J. A. Pople, M. Head-Gordon, *Chem. Phys. Lett.* **1989**, *157*, 479.
- [25] G. Kresse, J. Hafner, *Phys. Rev. B* **1993**, *47*, 558.
- [26] G. Kresse, J. Hafner, *Phys. Rev. B* **1994**, *49*, 14251.
- [27] G. Kresse, J. Furthmüller, *Phys. Rev. B* **1996**, *54*, 11169.
- [28] G. Kresse, J. Furthmüller, *Comput. Mater. Sci.* **1996**, *6*, 15.
- [29] P. E. Blöchl, *Phys. Rev. B* **1994**, *50*, 17953.
- [30] G. Kresse, D. Joubert, *Phys. Rev. B* **1999**, *59*, 1758.
- [31] J. P. Perdew, A. Ruzsinszky, G. I. Csonka, O. A. Vydrov, G. E. Scuseria, L. A. Constantin, X. Zhou, K. Burke, *Phys. Rev. Lett.* **2008**, *100*, 136406.
- [32] H. J. Monkhorst, J. D. Pack, *Phys. Rev. B* **1976**, *13*, 5188.
- [33] K. Momma, F. Izumi, *J. Appl. Cryst.* **2011**, *44*, 1272.
- [34] (a) J. P. Foster, F. Weinhold, *J. Am. Chem. Soc.* **1980**, *102*, 7211. (b) A. E. Reed, L. A. Curtiss, F. Weinhold, *Chem. Rev.* **1988**, *88*, 899.
- [35] (a) C. Kittel, *Introduction to Solid State Physics*, 8th ed., Wiley, Hoboken, NJ, **2005**, p. 50. (b) K. Kohlstedt, *ACS Cent. Sci.* **2016**, *2*, 278.
- [36] J. Emsley, *The Elements*, 2nd ed., Clarendon press, Oxford, **1991**.
- [37] A. B. Belonoshko, N. V. Skorodumova, A. Rosengren, B. Johansson, *Phys. Rev. B* **2006**, *73*, 012201.

Received: 23 November 2018

Revised: 3 March 2019

Accepted: 5 March 2019

Published online on 8 April 2019